

Summary Report of the FY-25 Reactor Physics Verification and Validation Exercises in the Advanced Reactor Technologies - Gas-Cooled Reactor Program

M3AT-25IN0603015

SEPTEMBER 2025

Zachary Prince,
Ishita Trivedi,
David Reger, and
Gerhard Strydom

Idaho National Laboratory

Carles Montoliu Lobo

North Carolina State University



DISCLAIMER

This information was prepared as an account of work sponsored by an agency of the U.S. Government. Neither the U.S. Government nor any agency thereof, nor any of their employees, makes any warranty, expressed or implied, or assumes any legal liability or responsibility for the accuracy, completeness, or usefulness, of any information, apparatus, product, or process disclosed, or represents that its use would not infringe privately owned rights. References herein to any specific commercial product, process, or service by trade name, trademark, manufacturer, or otherwise, does not necessarily constitute or imply its endorsement, recommendation, or favoring by the U.S. Government or any agency thereof. The views and opinions of authors expressed herein do not necessarily state or reflect those of the U.S. Government or any agency thereof.

Summary Report of the FY-25 Reactor Physics Verification and Validation Exercises in the Advanced Reactor Technologies - Gas-Cooled Reactor Program

M3AT-25IN0603015

**Zachary Prince,
Ishita Trivedi,
David Reger, and
Gerhard Strydom
Idaho National Laboratory
Carles Montoliu Lobo
North Carolina State University**

September 2025

**Idaho National Laboratory
INL ART Program
Idaho Falls, Idaho 83415**

<http://www.inl.gov>

**Prepared for the
U.S. Department of Energy
Office of Nuclear Energy
Under DOE Idaho Operations Office
Contract DE-AC07-05ID14517**

Page intentionally left blank

INL ART Program

**Summary Report of the FY-25 Reactor Physics
Verification and Validation Exercises in the Advanced
Reactor Technologies - Gas-Cooled Reactor Program**

INL/RPT-25-87443

September 2025

Technical Reviewer: (Confirmation of mathematical accuracy, and correctness of data and appropriateness of assumptions.)

Sinan Okyay

Sinan Okyay
Nuclear Engineer

Digitally signed by Sinan Okyay
Date: 2025.09.02 12:37:54 -06'00'

Date

Approved by:

KIP KLEIMENHAGEN (Affiliate)

Kip L. Kleimenhagen
ART Project Manager

Digitally signed by KIP KLEIMENHAGEN (Affiliate)
Date: 2025.09.02 15:17:47 -06'00'

Date

TRAVIS MITCHELL (Affiliate)

Travis R. Mitchell
ART Program Manager

Digitally signed by TRAVIS MITCHELL (Affiliate)
Date: 2025.09.03 07:19:21 -06'00'

Date

MICHELLE SHARP (Affiliate)

Michelle T. Sharp
INL Quality Assurance

Digitally signed by MICHELLE SHARP (Affiliate)
Date: 2025.09.02 13:35:42 -06'00'

Date

Page intentionally left blank

ABSTRACT

Validation and verification of numerical tools is critical for ensuring reasonable predictions for design scoping, licensing, and safety analyses. In this report, two reactor physics verification and validation exercises are presented. The first focuses on burnup analysis with data from the Advanced Gas Reactor (AGR) program. Simulations are performed with Monte Carlo N-Particle (MCNP), then compared with the measurements from the AGR-1 and -2 experiments that utilized both uranium oxycarbide (UCO) and uranium dioxide (UO₂) fuel. The second exercise utilizes data from the HTR-Proteus experiments to perform reactor physics validation. Specifications of the experimental facility are provided, along with a demonstration of initial modeling efforts in Serpent for one of the deterministic packing experiments. Both cases are part of the Generation-IV International Forum very-high-temperature reactor (VHTR) Computational Methods, Validation, and Benchmarking (CMVB) program, an international collaborative effort dedicated to verification and validation of high-temperature gas-cooled reactor (HTGR) analyses. Participation in the CMVB program allows the U.S. Department of Energy to leverage these existing validation activities in order to provide added value through benchmarking activities carried out in collaboration with other CMVB members.

Page intentionally left blank

ACKNOWLEDGMENTS

This research made use of Idaho National Laboratory's computing resources, which are supported by the U.S. Department of Energy's Office of Nuclear Energy and the Nuclear Science User Facilities under contract no. DE-AC07-05ID14517.

Page intentionally left blank

CONTENTS

ABSTRACT	v
ACKNOWLEDGMENTS	vii
ACRONYMS	xi
1. Depletion Validation with AGR-1 and AGR-2 data.....	1
1.1. Introduction	1
1.2. Experiment Description	1
1.3. Methodology	1
1.4. Results	2
2. Validation with HTR-Proteus.....	8
2.1. Introduction	8
2.2. Description of the HTR-PROTEUS Experiment.....	8
2.3. Methodology	8
2.4. Results	11
3. CONCLUSIONS	15
4. REFERENCES	17

FIGURES

Figure 1. AGR-1 and -2 depletion validation high-level workflow.....	2
Figure 2. AGR-1 and -2 depletion validation base MCNP model. Advanced Test Reactor (ATR) shown on the left; radial and axial cross section of the AGR-1 capsule shown on the right. The AGR-2 model looks identical, apart from the density of particles in the matrix.	3
Figure 3. Comparison of isotopic masses from the MCNP ORIGEN-S Activation Automation (MOAA) simulation to post-irradiation examination (PIE) measurements of the AGR-1 experiment.	3
Figure 4. Comparison of isotopic masses from the MOAA simulation to PIE measurements of the AGR-2 experiment. (The data for Capsules 1 and 4 are omitted due to the lack of published measurement data.).....	4
Figure 5. Burnup and fast neutron fluence time profiles for the AGR-1 and -2 experiments. The solid line shows the average of all the compacts, while the shaded region is the max/min compact values at that given time.	5
Figure 6. Isotopic concentration of select actinides and fission products versus burnup, from the AGR-1 MOAA results.	6

Figure 7. Isotopic concentration of select actinides and fission products versus burnup, from the AGR-2 MOAA results.	7
Figure 8. high-temperature reactor (HTR)-PROTEUS experiment core configure, showing the core cavity filled with pebbles [12].	9
Figure 9. Lattice cell configuration with hexagonal close-pack (HCP) [12].	9
Figure 10. Lattice cell configuration with columnar hexagonal point-on-point (CHPOP) [12]	10
Figure 11. Planar view of lattice cell layers in the CHPOP configuration. Each cell consists of three vertically stacked layers.	11
Figure 12. Radial view of the bottom three pebble layers in the Core 5 configuration of the HTR-PROTEUS experiment.	13
Figure 13. Radial view of the top-most pebble layer in the Core 5 configuration of the HTR-PROTEUS experiment.	14
Figure 14. HTR-PROTEUS Core 5 flux profile.	14

TABLES

Table 1. Eigenvalues obtained from Serpent for the HTR-PROTEUS Core 5 configuration.	12
Table 2. Reactivity corrections and relative differences.	15

ACRONYMS

AGR	Advanced Gas Reactor
ATR	Advanced Test Reactor
CHPOP	columnar hexagonal point-on-point
CMVB	Computational Methods, Validation, and Benchmarking
FIMA	fission per initial metal atom
HCP	hexagonal close-pack
HTGR	high-temperature gas-cooled reactor
HTR	high-temperature reactor
INL	Idaho National Laboratory
MCCAFE	Monte Carlo Constructor of ATR Fuel Elements
MCNP	Monte Carlo N-Particle
MOAA	MCNP ORIGEN-S Activation Automation
NDMAS	Nuclear Data Management and Analysis System
NEAMS	Nuclear Energy Advanced Modeling and Simulation
ORIGEN	Oak Ridge Isotope Generation code
OSCC	outer shim control cylinder
PIE	post-irradiation examination
SCALE	Standardized Computer Analyses Licensing Evaluation
TRISO	tri-structural isotropic
UCO	uranium oxycarbide
UO ₂	uranium dioxide
VHTR	very-high-temperature reactor

Page intentionally left blank

Summary Report of the FY-25 Reactor Physics Verification and Validation Exercises in the Advanced Reactor Technologies - Gas-Cooled Reactor Program

M3AT-25IN0603015

1. DEPLETION VALIDATION WITH AGR-1 AND AGR-2 DATA

1.1. Introduction

The first and second Advanced Gas Reactor (AGR) irradiation experiments, AGR-1 and AGR-2, involved particle irradiation tests conducted in the Advanced Test Reactor (ATR) at Idaho National Laboratory (INL). These experiments are part of a broader series of four tri-structural isotropic (TRISO) fuel irradiation experiments executed under the U.S. Department of Energy's Advanced Gas Reactor Fuel Development and Qualification Program, aimed at supporting development and deployment of the high-temperature gas-cooled reactors (HTGRs) that leverage advanced high-performance TRISO fuel.

The AGR experiments were designed with several explicit goals in mind: (1) providing irradiation performance data critical for fuel development, (2) generating irradiated fuel and material samples for comprehensive post-irradiation examination (PIE) and safety testing, (3) *validating fuel performance and fission product transport computational models and simulation tools*, and (4) qualifying fuel for normal operational scenarios anticipated in either prismatic-block or pebble-bed HTGR demonstration reactors.

Both the AGR-1 and AGR-2 irradiation experiments demonstrated exceptional performance. AGR-1 included ~20 wt% uranium oxycarbide (UCO) fuel kernels [1], achieving a maximum compact burnup of approximately 20% fission per initial metal atom (FIMA) and cumulative fast fluences approaching 4.5×10^{25} n/m² ($E_n > 0.18$ MeV) without any observed fuel particle failures [2]. AGR-2 tested both 14 wt% UCO and ~10 wt% uranium dioxide (UO₂) fuel kernels [3], again showing no evidence of fuel particle failure [4].

This milestone report documents the validation activities undertaken to evaluate the accuracy and reliability of computational tools utilized in simulating the AGR-1 and -2 experiments. Particular focus is placed on isotopic depletion modeling through the coupling of Monte Carlo N-Particle (MCNP) [5] with Oak Ridge Isotope Generation code (ORIGEN) [6]. The results of these simulations were compared with PIE measurements of isotopic concentrations in order to assess model fidelity. The subsequent sections of this report provide an overview of the methodology employed, detail the specific modeling approaches utilized, and present validation results. These efforts ensure robust verification of HTGR computational codes, methods, and modeling assumptions critical for supporting ongoing nuclear fuel development and qualification efforts.

1.2. Experiment Description

A detailed description of the AGR-1 experiment—with specifics related to isotopic depletion—can be found in [7]. The AGR-2 experiment is almost identical to AGR-1, with the primary differences lying in the fuel types and irradiation history, the details of which can be found in [3] and [4], respectively. The isotopic concentration measurements from PIE, which were the primary point of comparison for this work, were published in [8] and [9] for AGR-1 and -2, respectively.

1.3. Methodology

The depletion validation exercise for the AGR-1 and -2 experiments relies on three INL-based data management applications, along with the MCNP and Standardized Computer Analyses Licensing Evaluation

(SCALE)-ORIGEN physics codes. The workflow for the depletion validation is shown in Figure 1.

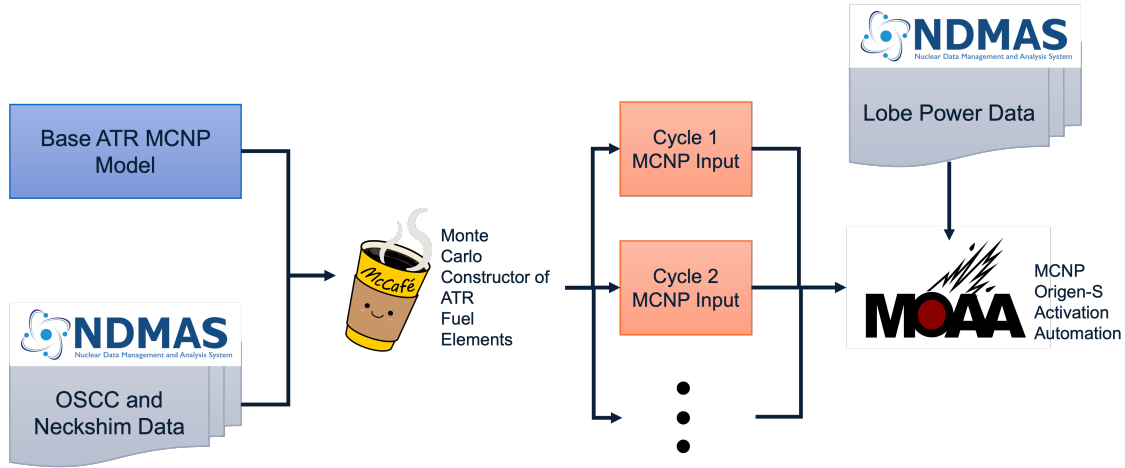


Figure 1. AGR-1 and -2 depletion validation high-level workflow.

The base ATR MCNP model was first developed with the experiment capsules included, as shown in Figure 2. Three of these models were developed, one for each of the experiment locations: B-10 (AGR-1), and B-12 and I-24 (AGR-2). Data on outer shim control cylinder (OSCC) and neckshim positions were gathered from the Nuclear Data Management and Analysis System (NDMAS). These data and the base model were put into Monte Carlo Constructor of ATR Fuel Elements (MCCAFE) [10] to produce an MCNP input file for each irradiation cycle. The startup, operation, and shutdown powers of each cycle were computed from NDMAS lobe power data. The MCNP inputs, power data, and compact cell numbers were specified in an MCNP ORIGEN-S Activation Automation (MOAA) [11] input, and executed to calculate the transient isotopic concentrations of the experiment. MOAA uses a coupled MCNP-ORIGEN predictor-corrector loop for each cycle’s time point (startup, operation, shutdown). It then outputs a full time history of isotopic mass, FIMA burnup, fast neutron flux/fluence, and neutron and gamma heating for each of the compacts and Hafnium shrouds. For the validation, the ORIGEN calculation outputs were compared to the PIE gamma spectrometry measurements.

1.4. Results

The gamma spectrometry measurements collected from the PIE emulate activity measures from end of compact irradiation plus one day. Six fission products were chosen for the analysis: Ce-144, Cs-134, Cs-137, Eu-154, Ru-106, and Zr-95. The published data from AGR-2 include uncertainty estimates regarding the measurement. Figure 3 and Figure 4 show the results of MOAA simulation with the AGR-1 and -2 data, respectively. These figures show, for each compact, the relative difference between the measurement and simulation, with “Total” at the far right being the sum of all the compacts, computed as:

$$\frac{M_i^{\text{calculated}} - M_i^{\text{measurement}}}{M_i^{\text{measurement}}}, \quad (1)$$

where M_i is the mass of isotope i in the compact.

The AGR-1 results in Figure 3 show decent agreement with measurements for higher-concentration fission products such as Cs-137 and Ce-144. However, large differences can be observed for Cs-134 and Eu-154, especially in Capsule 6. However, these differences seem to cancel out for the total error. Whether the difference is positive or negative seems to depend primarily on the radial location (stack) of

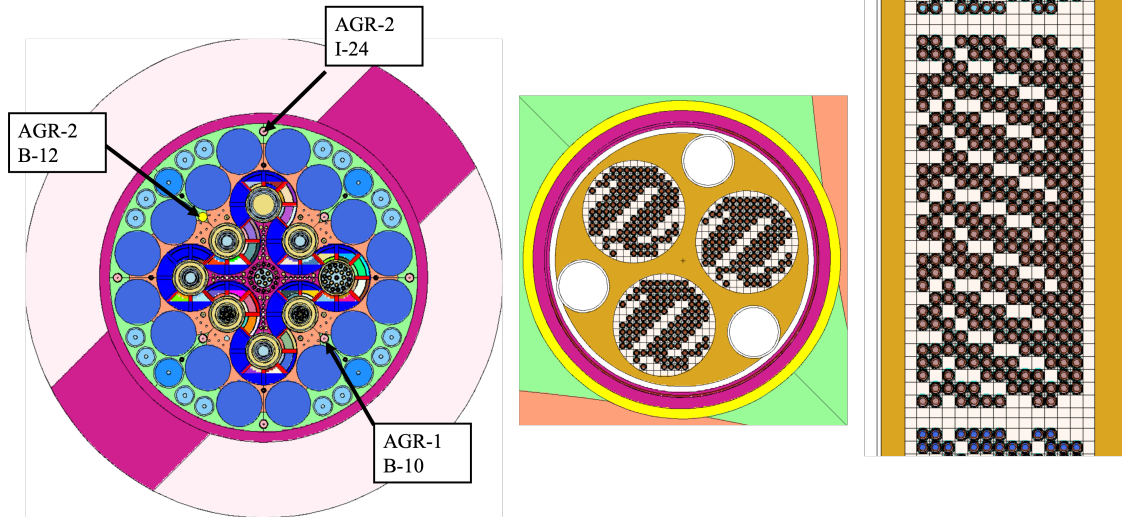


Figure 2. AGR-1 and -2 depletion validation base MCNP model. ATR shown on the left; radial and axial cross section of the AGR-1 capsule shown on the right. The AGR-2 model looks identical, apart from the density of particles in the matrix.

the compact in the capsule, whereas the magnitude of the difference appears to depend on the axial location (capsule/layer). Further sensitivity analysis needs to be performed on the model to understand this behavior, as one source of uncertainty in the model is the effect of other experiments also in the reactor. When it comes to lower-concentration isotopes, the AGR-2 results in Figure 4 show a smaller amount of deviation from the measurements than does AGR-1, yet they still retain decent agreement with the higher-concentration isotopes. The differences do not reflect the same radial dependence as AGR-1, though a similar axial dependence is observed.

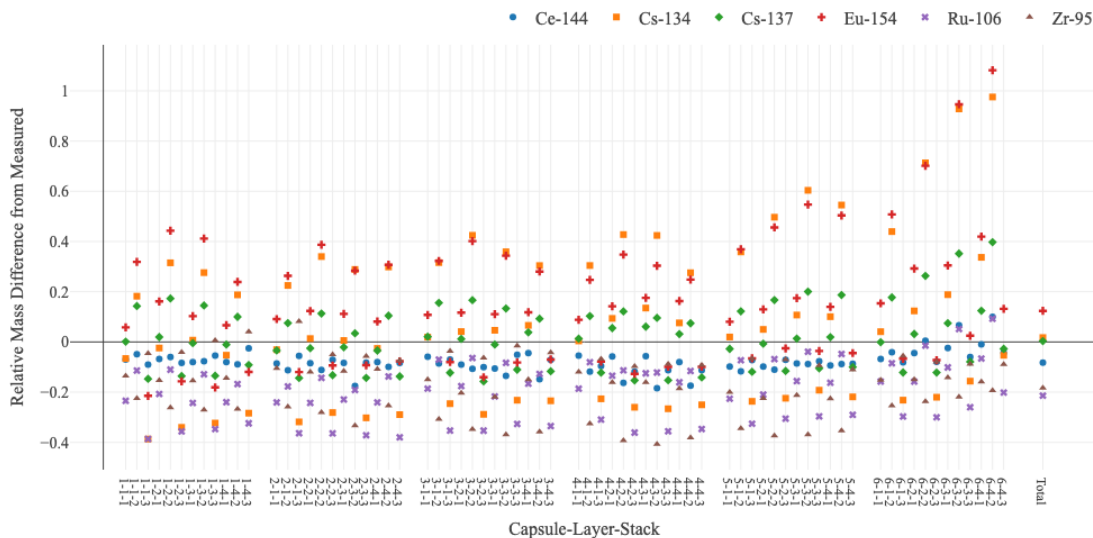


Figure 3. Comparison of isotopic masses from the MOAA simulation to PIE measurements of the AGR-1 experiment.

The results from MOAA offer much more that can be used for code-to-code comparison. This includes

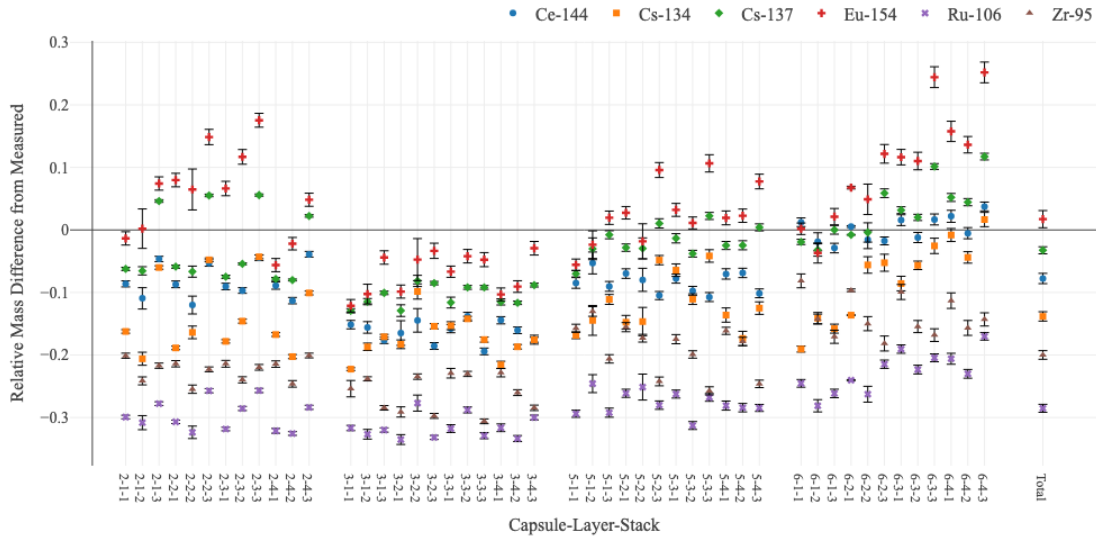


Figure 4. Comparison of isotopic masses from the MOAA simulation to PIE measurements of the AGR-2 experiment. (The data for Capsules 1 and 4 are omitted due to the lack of published measurement data.)

burnup and fast-fluence profiles, such as that shown in Figure 5. Additionally, burnup dependence on actinides and fission products can be compared, based on the profiles shown in Figure 6 and Figure 7. The colors in Figure 7 are intentional, with blue and red representing the UO₂ and UCO fuel kernels, respectively. This distinction helps show the profile differences in the isotope concentration when comparing different fuel types, indicating the importance of considering initial TRISO particle composition when determining fission product accumulation.

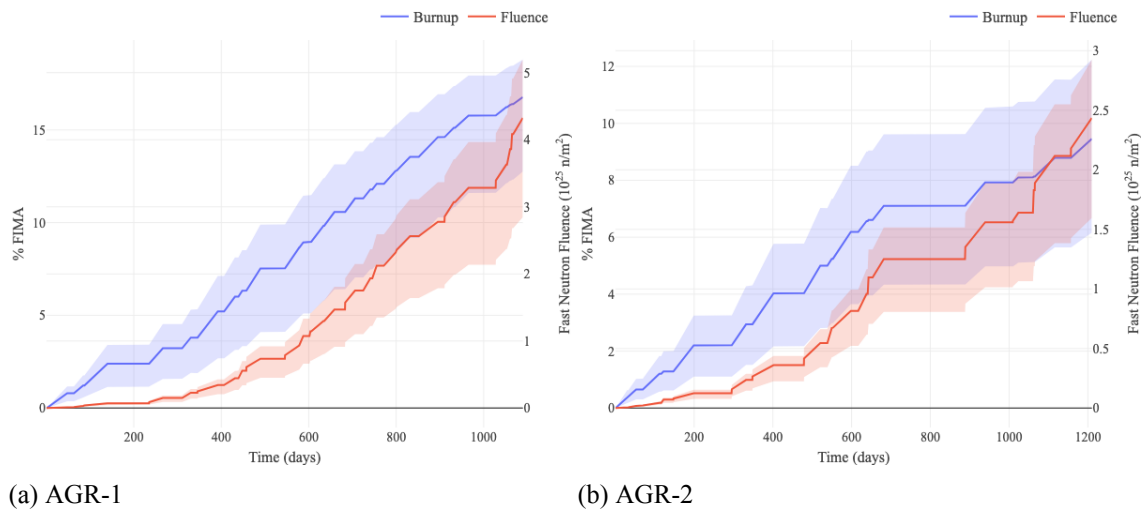


Figure 5. Burnup and fast neutron fluence time profiles for the AGR-1 and -2 experiments. The solid line shows the average of all the compacts, while the shaded region is the max/min compact values at that given time.

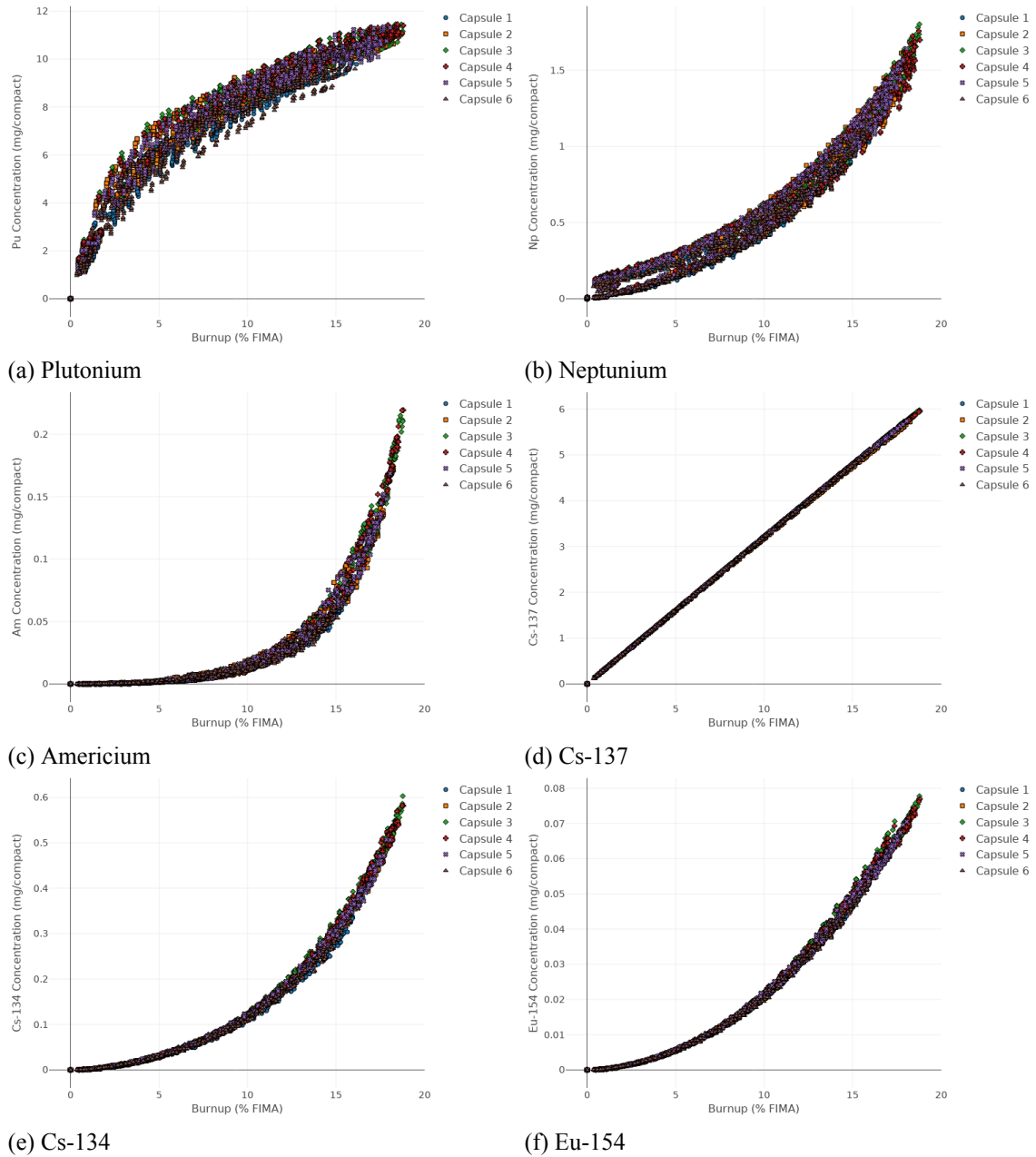
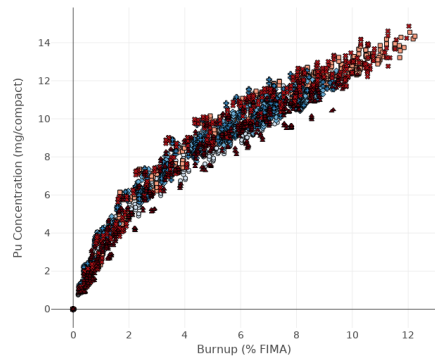
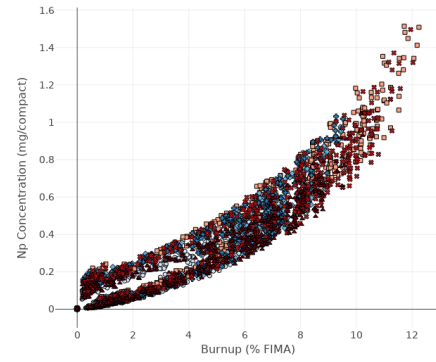


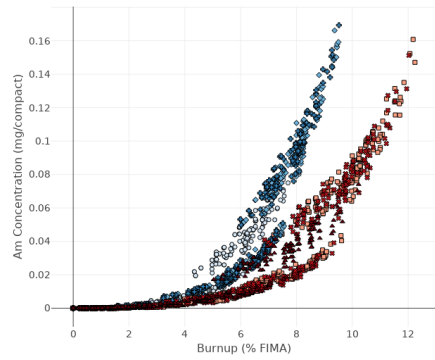
Figure 6. Isotopic concentration of select actinides and fission products versus burnup, from the AGR-1 MOAA results.



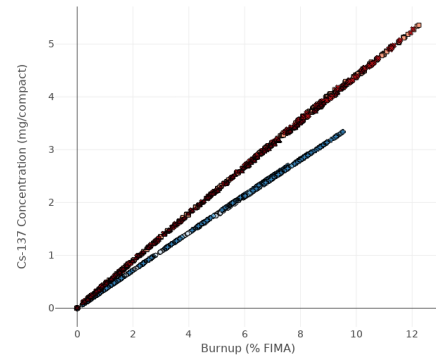
(a) Plutonium



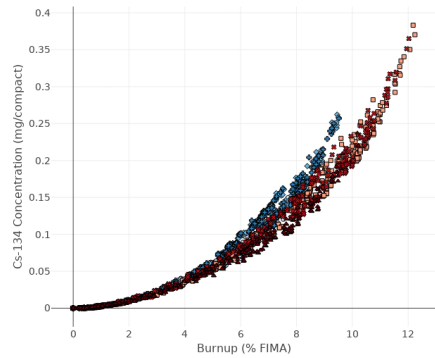
(b) Neptunium



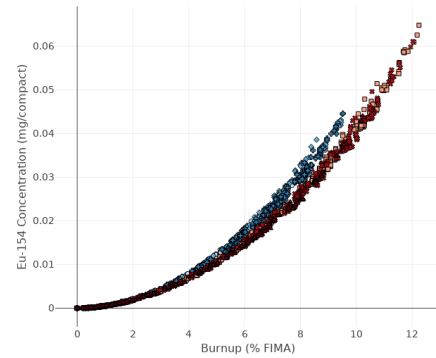
(c) Americium



(d) Cs-137



(e) Cs-134



(f) Eu-154

Figure 7. Isotopic concentration of select actinides and fission products versus burnup, from the AGR-2 MOAA results.

2. VALIDATION WITH HTR-PROTEUS

2.1. Introduction

The high-temperature reactor (HTR)-PROTEUS experiment program is a key effort in validating computational tools for very-high-temperature reactors (VHTRs) [12]. These experiments were conducted to provide experimental data for benchmarking reactor physics tools usable to analyze HTRs. Among the measured data were the criticality measurement, differential and integral control/safety rod worth, kinetics parameters, reaction rates, water ingress effects, and sample reactivity effects [12]. This section of the milestone report summarizes the efforts made toward developing a Generation-IV International Forum validation benchmark to assess variations in key safety and performance parameters resulting from the random distribution of particles and pebbles in a pebble-bed reactor. The work is being pursued in three stages: (1) developing benchmark specifications for all configurations of the HTR-PROTEUS core discussed in [12], [13], [14] and, [15]; (2) developing benchmark exercises for assessing the stochastic core configuration in order to quantify uncertainties in the core reactivity, pebble power, and temperature distributions resulting from the stochastic variations in pebble and particle distributions; and (3) assimilating data from signatories. This report highlights the work completed toward finalizing the specifications (Stage 1).

2.2. Description of the HTR-PROTEUS Experiment

PROTEUS is a zero-power research reactor that features a cylindrical graphite annulus core with a central cylindrical cavity, as illustrated in Figure 8. The core is surrounded by graphite radial reflectors. The contents of the annulus are determined by the experiment of interest. For the HTR-PROTEUS experiments, the central cavity was configured as a pebble-bed reactor using TRISO fuel, whereas UO_2 fuel was dispersed in a graphite pebble. Ten different core configurations were considered in the PROTEUS experiments, as detailed in [12]. The pebbles were packed deterministically for all core configurations except Core 4, which was packed randomly in the manner described in [13]. The pebble lattices for the deterministic cores were configured using either the hexagonal close-pack (HCP) (Figure 9) or columnar hexagonal point-on-point (CHPOP) (Figure 10) configurations [12].

The pebble packing fraction for the HCP and CHPOP configurations is 0.7405 and 0.6046, respectively as noted in [12]. The random packing configuration was approximated to have a packing fraction of 0.61 [16]. Additional details on the core design and specifications can be found in [12], [13], [14], and, [15].

2.3. Methodology

The reference solutions for the cores were developed using the Monte Carlo tool Serpent, version 2.1, which is a continuous energy neutron and photon transport code developed at VTT in Finland [17]. The HTR-PROTEUS specifications include reference solutions for core criticality, power distribution, reaction rates, control rod worth, and kinetics parameters so as to enable comparison of results among benchmark participants.

The TRISO particles in each pebble were explicitly modeled and randomly distributed in the graphite matrix by using the *disperse* utility in Serpent [18]. Serpent can generate the random particle locations as Cartesian coordinates by using a predefined packing fraction. This file is then called into the main Serpent input to allocate the location of each TRISO particle inside a fuel pebble, using the *pbcd* card in Serpent [18]. In the Serpent models, each case consists of 500,000 neutrons per cycle, with 500 active cycles and 100 inactive cycles being implemented in order to maintain less than 10 pcm of uncertainty on the eigenvalue. The unresolved resonances were activated and the core power was set to 1 kW. The ENDF/B-VIII.0 [19] cross-section library was used to obtain the cross-section data and associated S(alpha,beta) libraries at 294 K.

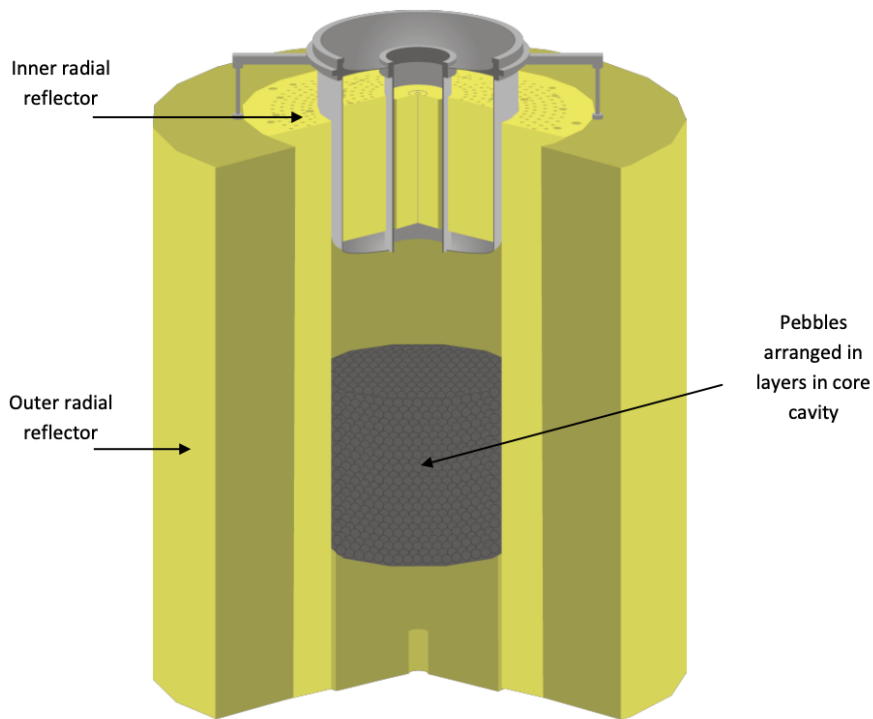


Figure 8. HTR-PROTEUS experiment core configure, showing the core cavity filled with pebbles [12].

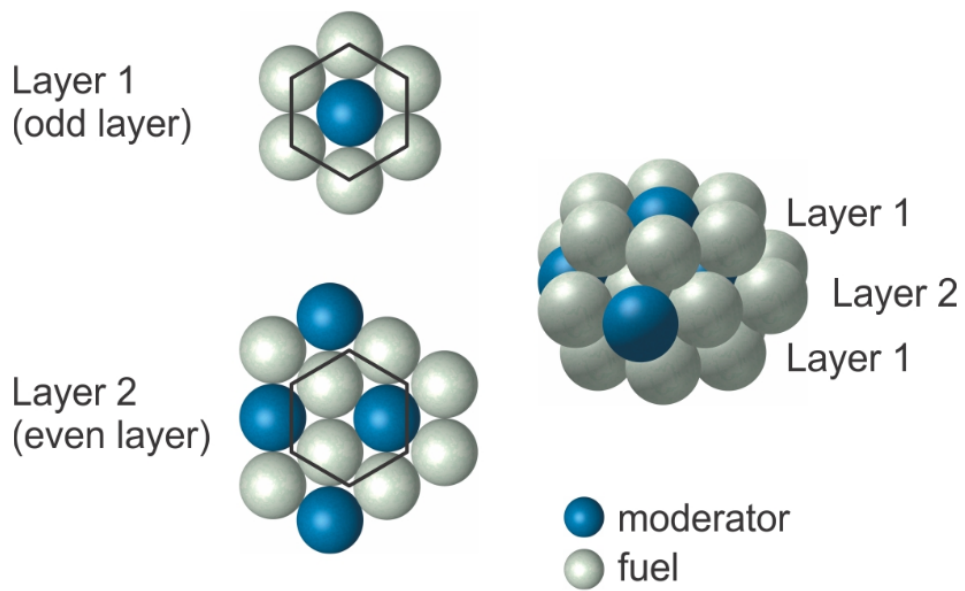


Figure 9. Lattice cell configuration with HCP [12].

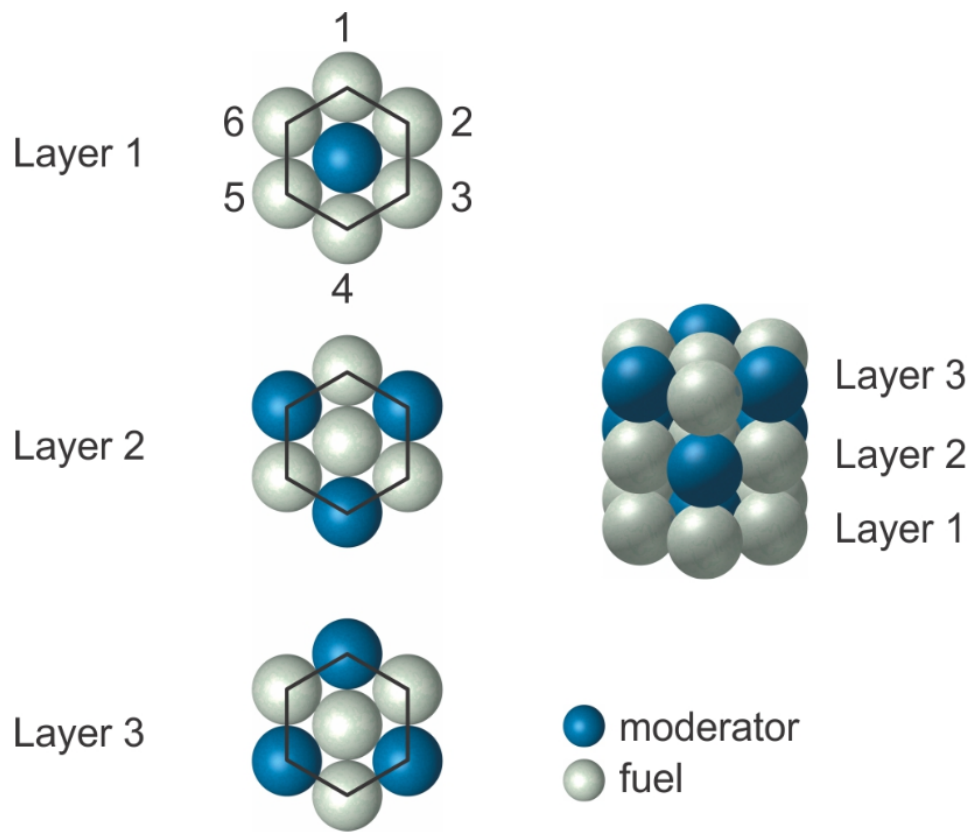


Figure 10. Lattice cell configuration with CHPOP [12]

2.4. Results

This section gives the preliminary results for the Core 5 configuration, which follows the CHPOP cell lattice. Figure 11 illustrates utilization of the *disperse* and *pbed* utilities for generating the Core 5 CHPOP lattice configuration, shown in Figure 11.

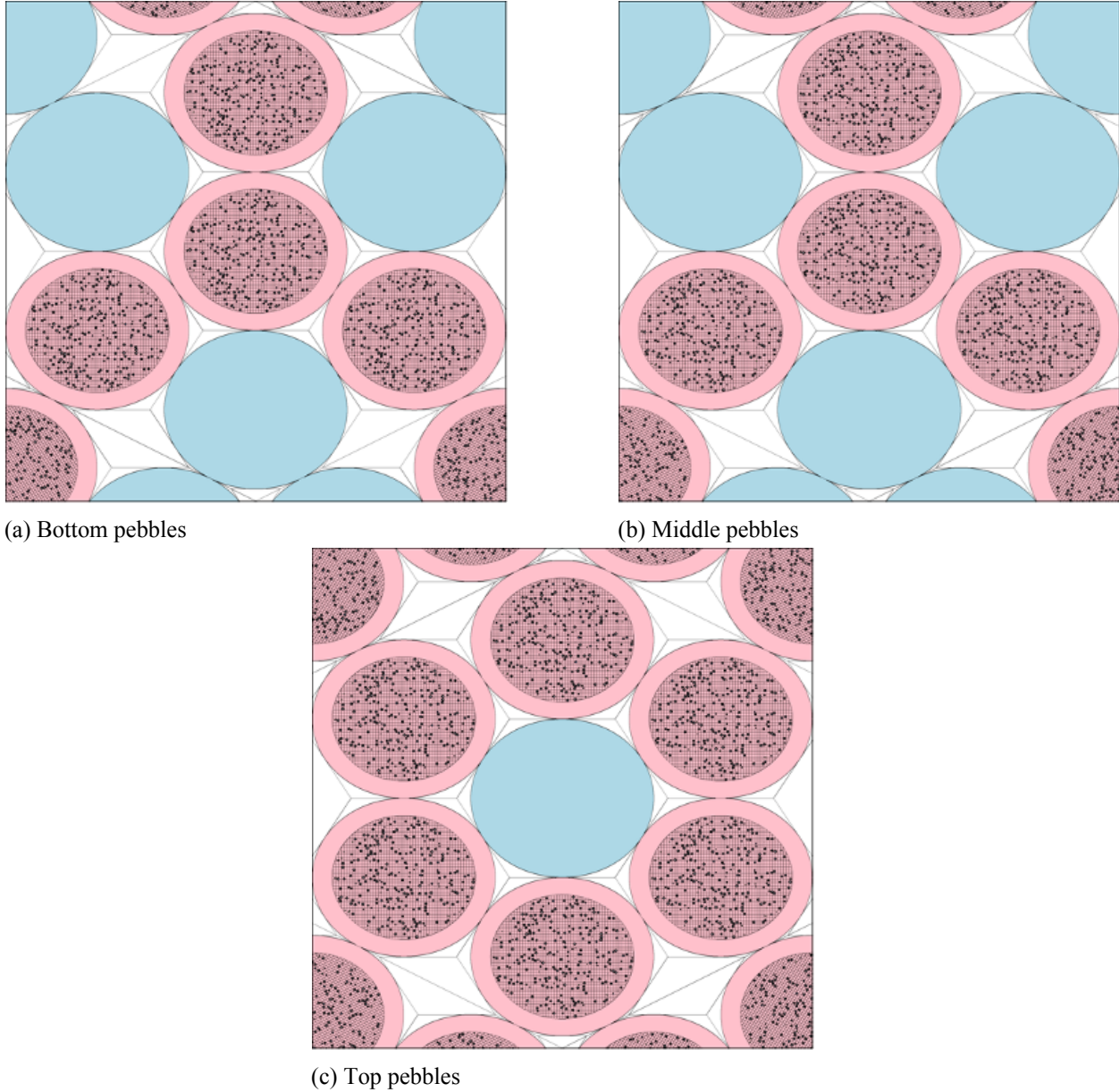


Figure 11. Planar view of lattice cell layers in the CHPOP configuration. Each cell consists of three vertically stacked layers.

The reactor model comprises a central core cavity, two axial reflectors (located above and below the core cavity), and a radial reflector that included four control rods, eight safety/shutdown control rods, and a unique autorod [14]. An important modeling approximation was applied to the autorod model in Serpent. Since the autorod is tapered along its length [12], the geometry is homogenized inside the autorod insertion hole, making modeling simpler.

The central core cavity was a cylinder 125.7 cm in diameter and 189.3 cm in height. Core 5 had a 1:2 moderator-to-fuel-pebble ratio, with a total of 2,870 moderator graphite pebbles and 5,433 fuel pebbles organized into 23 layers, forming a stack 138 cm high from the bottom of the cavity, using CHPOP cell configuration.

The bottom three pebble layers in the core lattice structures are described in Figure 11a (bottom layer), Figure 11b (second layer), and Figure 11c (third layer). These three layers (shown in Figure 12) were stacked consecutively to serve as the initial layers of the critical height. This triple layer structure was replicated another six times, and these replicated layers were then stacked on top of the initial set, for a total of 21 layers.

The last two (top-most) layers repeated layer 1, followed by a different pebble distribution (shown in Figure 13). Graphite fillers were positioned inside the cylindrical cavity, creating a dodecagon to preserve the lattice configuration and prevent shaking of pebbles. Reactivity control was achieved using four stainless-steel control rods and a tapering copper-plate autorod while the borated stainless-steel safety/shutdown rods remained fully withdrawn from the core. These were identified as the circular holes surrounding the central cylinder in Figure 12 and Figure 13. Additional design specifications on Core 5 can be found in [14].

For the initial calculations, three different Core 5 reactor states from [14] were modeled:

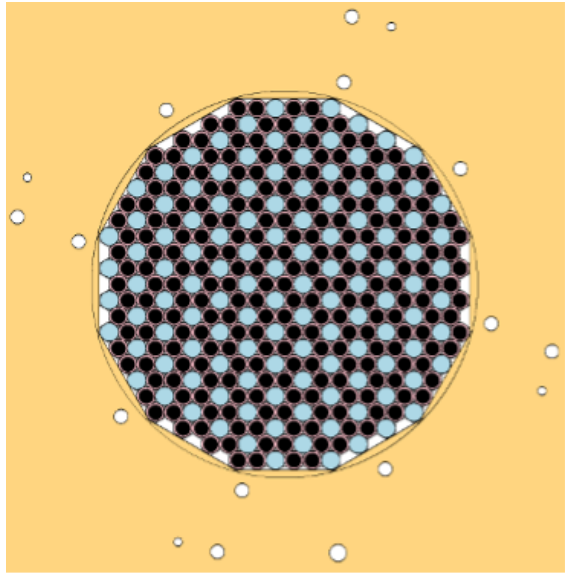
1. State 5.1: Coolant channels are open to air under standard operating conditions. Control and safety rods are partially inserted.
2. State 5.2: Coolant channels are filled with graphite plugs. Control rods are partially inserted.
3. State 5.3: Coolant channels are filled with graphite plugs. Control rods are partially inserted at an insertion depth different from that in State 5.2.

Per the preliminary results, the thermalized flux profile for Core 5 (state 5.1) is shown in Figure 14. Table 1 shows the preliminary eigenvalue results from Serpent which can be compared with experimental critical eigenvalue of 1.0000 ± 0.0030 for core 5 configurations [14]. Although all computed values fall outside the experimental uncertainty of 300 pcm, State 5.1 shows the largest deviation from the experimental value (i.e., 1,232 pcm), while States 5.2 and 5.3 show a difference of 796 and 838 pcm from the measured value, respectively.

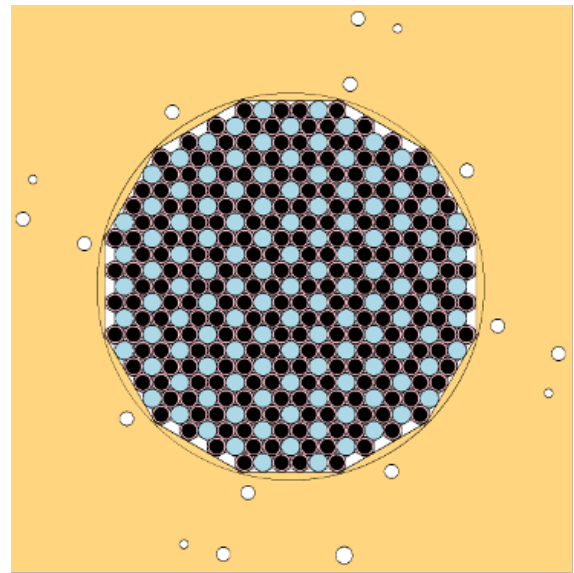
Table 1. Eigenvalues obtained from Serpent for the HTR-PROTEUS Core 5 configuration.

Core State	Computed Eigenvalue	Monte Carlo Uncertainty, pcm
5.1	0.984680	6.1
5.2	0.989043	6.1
5.3	0.988620	5.9

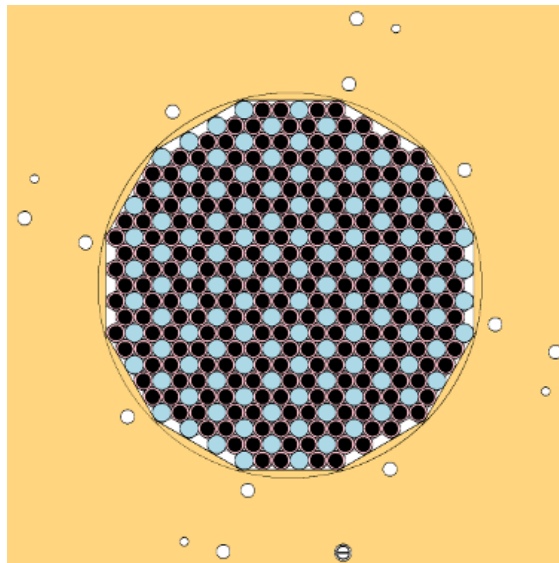
Since all three states utilize both control rods and an autorod, individual reactivity correction for each rod type was evaluated (see Table 2). When comparing against the experimental data, the large differences between reactivity insertion from the autorod suggests biases in our results, stemming from approximated autorod models. This also likely leads to a large deviation from criticality. Further improvements in autorod modeling are needed to investigate the cause of these deviations.



(a) Layer 1



(b) Layer 2



(c) Layer 3

Figure 12. Radial view of the bottom three pebble layers in the Core 5 configuration of the HTR-PROTEUS experiment.

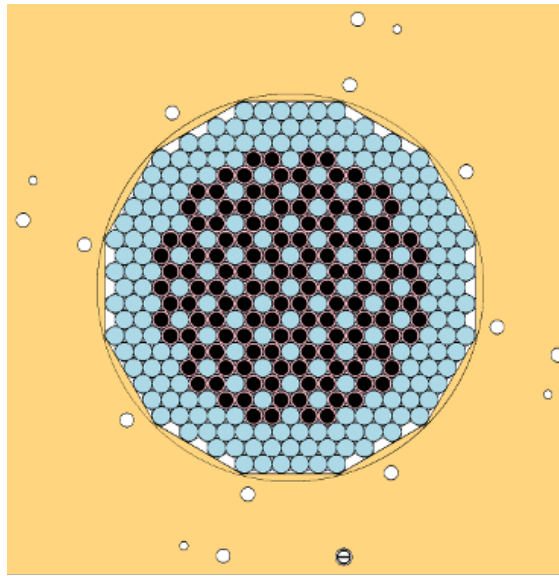


Figure 13. Radial view of the top-most pebble layer in the Core 5 configuration of the HTR-PROTEUS experiment.

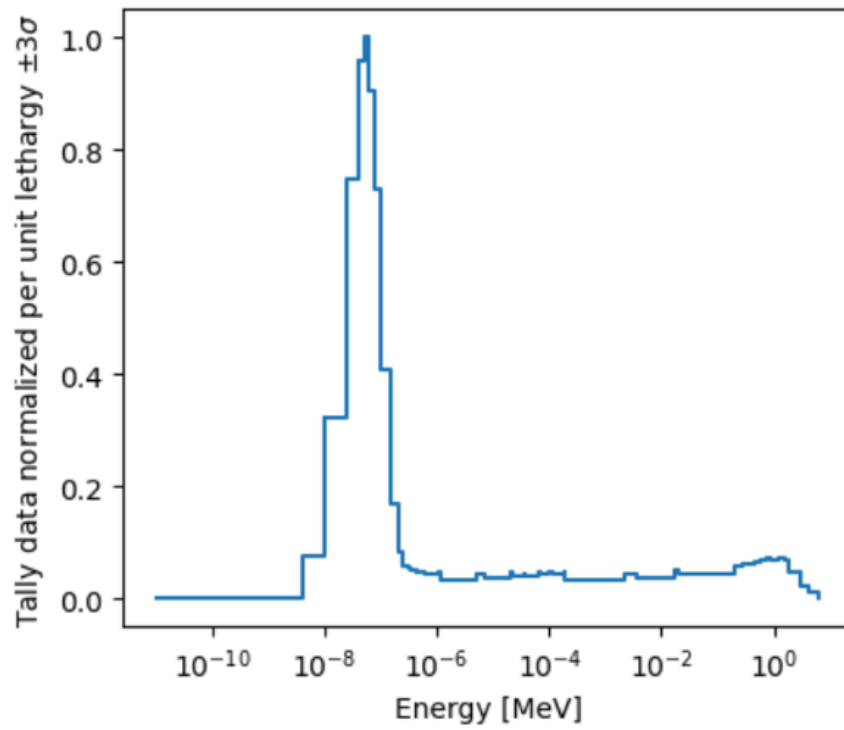


Figure 14. HTR-PROTEUS Core 5 flux profile.

Table 2. Reactivity corrections and relative differences.

Core	Rod Correction	Reactivity Correction (ρ)	Experimental Reactivity Correction (ρ)	Relative Difference
5.1	Control rod insertion (181.5 cm)	-68.504	-68.8 ± 1	0.4302 %
	Autorod insertion (12 cm)	-5.2	-1.3 ± 0.2	300.00 %
5.2	Control rod insertion (5.5 cm)	-84.187	-84.2 ± 1	0.0154 %
	Autorod insertion (94.4 cm)	-1.784	-0.6 ± 0.2	197.33 %
5.3	Control rod insertion (194.5 cm)	-84.187	-84.2 ± 1	0.0154 %
	Autorod insertion (17 cm)	-7.872	-1.7 ± 0.2	363.06 %

3. CONCLUSIONS

Depletion validation of the AGR-1 and -2 irradiation experiments demonstrated the effectiveness of a robust modeling and simulation workflow that integrates INL-developed data tools with the MCNP and SCALE-ORIGEN physics codes. By leveraging historical operating data and a detailed full-core ATR model, the MOAA framework successfully simulated transient isotopic concentrations and enabled direct comparison with PIE gamma spectrometry measurements. The validation results showed generally good agreement for high-activity fission products such as Cs-137 and Ce-144, while larger deviations for isotopes such as Cs-134 and Eu-154 highlighted sensitivities tied to compact positioning and capsule layer. AGR-2 results, particularly for lower-concentration isotopes, displayed improved consistency with measurements compared to AGR-1. Additionally, the distinction in depletion behavior between UCO and UO₂ fuel types underscores the importance of accounting for initial fuel composition in modeling efforts. These results not only contribute to the validation of the coupled MCNP-ORIGEN depletion methodology, but also provide a foundation for future sensitivity studies and code-to-code comparisons, further supporting the qualification of TRISO fuel and modeling tools for HTGR applications. Avenues of future work could include (1) improving the base MCNP model through depletion of the fuel elements during each cycle, (2) performing sensitivity analyses on uncertain experimental parameters, (3) quantifying model-form uncertainty, and (4) performing code-to-code comparisons with Nuclear Energy Advanced Modeling and Simulation (NEAMS) tools.

The HTR-PROTEUS experimental program is crucial for validating computational tools for VHTR analysis. The structured benchmark efforts are aimed at quantifying the uncertainties in core reactivity and power distribution that are caused by stochastic variations in pebble arrangements. This report provided an overview of the initial phase of these efforts, focusing on the Core 5 configuration using the CHPOP cell lattice.

The preliminary results, obtained via the Serpent Monte Carlo code, highlight significant deviations in calculated eigenvalues and reactivity corrections when comparing against experimental data. The largest discrepancy was observed for State 5.1—namely, an eigenvalue deviation of 1,232 pcm. Detailed analysis revealed that the autorod model, particularly the reactivity insertion corrections, exhibited considerable biases contributing to these deviations.

Moving forward, it is essential that the autorod model be refined to address these discrepancies. Such improvements will enhance the accuracy of the computational tools, ensuring reliable predictions regarding the safety and performance parameters of VHTRs. Continued collaboration and data assimilation from all signatories will be pivotal for achieving the final benchmark specifications and exercises.

Page intentionally left blank

4. REFERENCES

- [1] J. T. Maki, “AGR-1 irradiation experiment test plan,” Tech. Rep. INL/EXT-05-00593, Idaho National Laboratory (INL), Oct. 2009.
- [2] B. P. Collin, “AGR-1 irradiation test final as-run report, rev. 3,” Tech. Rep. INL/EXT-10-18097, Idaho National Laboratory (INL), Dec. 2014.
- [3] B. P. Collin, “AGR-2 irradiation experiment test plan,” Tech. Rep. PLN-3798, Idaho National Laboratory (INL), Oct. 2011.
- [4] B. P. Collin, “AGR-2 irradiation test final as-run report (revision 4),” Tech. Rep. INL/EXT-14-32277-Rev004, Idaho National Laboratory (INL), Idaho Falls, ID (United States), Jan. 2018.
- [5] F. B. Brown, “Advanced computational methods for monte carlo calculations,” Presentation LA-UR-18-20247, Los Alamos National Laboratory, Los Alamos, NM, USA, 2018.
- [6] M. J. Bell, “ORIGEN: the ORNL isotope generation and depletion code,” Tech. Rep. ORNL-4628, Oak Ridge National Laboratory, May 1973.
- [7] J. W. Sterbentz and J. J. Cogliati, “AGR-1 depletion benchmark,” Tech. Rep. INL/EXT-18-45840, Idaho National Lab. (INL), July 2018.
- [8] J. M. Harp, “Analysis of individual compact fission product inventory and burnup for the AGR-1 TRISO experiment using gamma spectrometry,” Tech. Rep. ECAR-1682, Idaho National Laboratory, 2014.
- [9] J. M. Harp, J. D. Stempien, and P. A. Demkowicz, “Fission product inventory and burnup evaluation of the AGR-2 irradiation by gamma spectrometry,” Tech. Rep. INL/EXT-16-39777, Idaho National Laboratory (INL), Sept. 2016.
- [10] T. Labossiere-Hickman, “MCCAFE: The monte carlo constructor for ATR fuel elements,” *Transactions of the American Nuclear Society*, vol. 131, no. 1, pp. 610–611, 2024. 2024 Transactions of the American Nuclear Society on Winter Conference and Expo, ANS 2024 ; Conference date: 17-11-2024 Through 21-11-2024.
- [11] R. E. Fairhurst-Agosta, A. L. Carter, and J. L. Peterson-Droogh, “Development of the MCNP-ORIGEN activation automation tool,” in *Proceedings of the International Conference on Physics of Reactors, PHYSOR 2022*, pp. 1923–1932, American Nuclear Society, 2022.
- [12] J. D. Bess, B. H. Dolphin, J. W. Sterbentz, L. Snoj, I. Lengar, O. Köberl, and J. Kelly, “HTR-PROTEUS pebble bed experimental program cores 1, 1a, 2, and 3: Hexagonal close packing with a 1:2 moderator-to-fuel pebble ratio (rev. 1),” Tech. Rep. INL/EXT-11-23219, Idaho National Laboratory (INL), Idaho Falls, ID (United States), Feb. 2013.
- [13] J. D. Bess, L. M. Montierth, J. W. Sterbentz, J. B. Briggs, H. D. Gougar, L. Snoj, I. Lengar, and O. Koberl, “HTR-PROTEUS pebble bed experimental program core 4: random packing with a 1:1 moderator-to-fuel pebble ratio,” Tech. Rep. INL/EXT-12-27057, Idaho National Lab. (INL), Idaho Falls, ID (United States), Feb. 2014.
- [14] J. D. Bess, J. W. Sterbentz, L. Snoj, I. Lengar, and O. Koberl, “HTR-PROTEUS pebble bed experimental program cores 5,6,7,&8: Columnar hexagonal point-on-point packing with a 1:2 moderator-to-fuel pebble ratio,” Tech. Rep. INL/EXT-12-26585, Idaho National Laboratory (INL), Idaho Falls, ID (United States), Feb. 2015.

- [15] J. D. Bess, “HTR-PROTEUS pebble bed experimental program cores 9 & 10: columnar hexagonal point-on-point packing with a 1:1 moderator-to-fuel pebble ratio,” Tech. Rep. INL/EXT-12-25334, Idaho National Lab. (INL), Idaho Falls, ID (United States), Feb. 2014.
- [16] F. C. Difulippo, “Monte carlo calculations of pebble bed benchmark configurations of the PROTEUS facility,” *Nuclear Science and Engineering*, vol. 143, no. 3, pp. 240–253, 2003.
- [17] J. Leppänen, V. Valtavirta, A. Rintala, and R. Tuominen, “Status of serpent monte carlo code in 2024,” *EPJ - Nuclear Sciences & Technologies*, vol. 11, 2025.
- [18] V. Rintala, H. Suikkanen, J. Leppänen, and R. Kyrki-Rajamäki, “Modeling of realistic pebble bed reactor geometries using the serpent monte carlo code,” *Annals of Nuclear Energy*, vol. 77, pp. 223–230, 2015.
- [19] G. Nobre and D. Brown, “ENDF B-VIII.1 full library,” Oct. 2024.